Shear Strength and Stiffness Degradation of Geomaterials in Cyclic Loading

R. Pytlik, S. Van Baars

Abstract. Cyclic loading on civil structures can lead to a reduction of strength and stiffness in the loaded materials. The life span of many cyclically loaded structures such as wind turbines, high-speed train tracks and bridges strongly depends on the foundation. The soils and rocks in the foundation can be subjected to cyclic loads from natural and human sources. In order to evaluate the fatigue behaviour of geomaterials, this paper presents static and cyclic triaxial test results for several geomaterials. It was concluded that cyclic loading on different geomaterials can cause different types of effects. The shear strength of cohesionless crumbled limestone increases during cyclic loading; while for cohesive materials, such as gypsum and mortar, the strength decreases. The strength decrease can be seen as a degradation of the cohesion. The most significant factor in the cohesion reduction was found to be the number of applied cycles. It was also noticed that the friction angle for sands does not reduce under cyclic loading. A fatigue limit was not found for cohesive geomaterials; neither a dependence of the strength reduction on the cyclic loading ratios.

Keywords: geomaterials, cyclic loading, fatigue, foundation, strength reduction, stiffness reduction.

1. Introduction

The life span of many structures, such as wind turbines, high-speed trains or bridges etc., depends on the fatigue behaviour of the foundation and the surrounding ground mass. An analysis of these structures requires careful planning at the initial stage and a good evaluation of the degradation process in cyclic loading. The impact of the acting forces, both constant and variable, must be taken into account to estimate the strength and stability of the whole structure. Variable forces, due to the repetitive nature of the loads, are known as a cyclic loading, and can significantly reduce the strength and stiffness of materials and lead to an accumulation of strains. Failure of a material due to cyclic loading is known as 'fatigue'.

The fatigue of the ground is an important mechanism in foundation designs. However, this mechanism has not yet been fully investigated. Except for a limited number of researchers and a few design guidelines for the offshore oil and gas industry (*e.g.* the American Petroleum Institute Recommended Practice - API RP,(2000); or Det Norske Veritas (DNV, 2013), there is no typical civil engineering procedure that describes the effects of cyclic loading on soil and rocks. So far, the most detailed description of the strength reduction due to cyclic loading exists in the field of earthquake engineering (*i.e.* Eurocode 8: Design of structures for earthquake resistance, Part 5, 2004). Yet this procedure is rather unsuitable to adapt for areas where earthquakes do not occur. Even more, the safety factors applied in earthquake engineering are very high, and thus impractical for normal conditions.

Another method for predicting the fatigue of geomaterials is to use the available theoretical models. However, the only available models for cyclic damage that exist in geotechnical engineering focus on the following three aspects: the strain-stress behaviour of the soil, the increase in pore water pressure, and the pile shaft friction degradation.

The stress-strain behaviour has already been investigated by many researchers. To mention only a few of them: Seed & Lee(1966), Matlock *et al.* (1978), Ibsen(1999) and Andersen *et al.* (2013). As these studies focus mainly on strain accumulation, they are not useful for estimating the remaining shear strength. The other limitations of these methods are that they are difficult to use, require many parameters, and cannot be applied for all geomaterials (*e.g.* the model given by Niemunis *et al.*, 2005).

In undrained soils, cyclic loading may generate a high pore pressure which leads to a loss of bearing capacity of foundations by liquefaction (*e.g.* foundations of off-shore wind power turbines, or costal piers). Some formulas to calculate the increase of pore pressure are given by Seed *et al.* (1976), Lee & Albesia(1974) and the DeAlba *et al.* (1976). In order to optimise the control of the effective stresses, all laboratory tests were unsaturated. Thus, the changes in pore pressure due to cyclic loading were omitted.

Currently, no model exists which describes the reduction of the shear strength of geomaterials due to cyclic loading. In order to describe the loss of shear strength due to cyclic loading, and to determine the design values of the soil strength parameters, a proper strength reduction model for both rock and soils is needed. Such a model should pre-

Robert Pytlik, PhD. Student, Faculty of Science, Technology and Communication, University of Luxembourg, Luxembourg, e-mail: PytlikRobert@gmail.com.
Stefan Van Baars, PhD., Full Professor, Faculty of Science, Technology and Communication, University of Luxembourg, Luxembourg, e-mail: Stefan.VanBaars@uni.lu.
Submitted on November 25, 2015; Final Acceptance on November 27, 2016; Discussion open until April 28, 2017.

dict the loss of strength as a function of the number of cycles under cyclic loading, including probability bands in cases where a correct evaluation of the remaining strength and life of geomaterials is required.

2. Shear Strength Degradation

For evaluation of the strength degradation in metals due to cyclic loading a couple of approaches are widely used. The most common approaches include: the simplistic approach (*e.g.* the Palmgren-Miner rule); the damage mechanics approach (*e.g.* Lemaitre brittle damage model); fracture mechanics approach (*e.g.* Paris' Law); the phenomenological (empirical) approach (S-N curve); the remaining strength approach, and others. All of these are well described and have been confirmed in multiple tests (see for example: Pook, 2007).

The Palmgren-Miner rule is a linear damage hypothesis for which failure occurs when the damage parameter reaches a certain value. According to this rule, the damage accumulates linearly with the number of stress cycles, which is usually not true. The Paris law describes the crack growth in cyclic loading based on empirical correlations. The continuum damage mechanics models use state variables to represent the effects of damage on the material, based on *e.g.* thermodynamical aspects of cyclic loading. The most commonly used method for describing fatigue is the phenomenological approach. Therefore, it was decided to apply this approach also to rock and soil mechanics.

In this paper, two, quite similar, approaches for the fatigue tests are investigated and compared:

- the S-N approach
- the remaining strength approach

The basic methodology for these two approaches is the assumption that the initial static strength S_0 will be reduced after N cycles of σ_{cyc} loading.

2.1. S-N approach

The main purpose of the S-N approach is to count the number of cycles N for a given cyclic stress level σ_{cyc}, until the sample reaches a failure state. The failure state is observed when the material is not able to reach the applied cyclic stress level σ_{cyc} anymore. This simply states that the static strength S_0 is reduced to σ_{cyc} for the last cycle N, where N is the sought variable denoting the life of the material at a given cyclic stress level σ_{cyc}. Thus, a single "S-N" curve can be created for each cyclic load σ_{cyc} (S in the S-N formula), and for the corresponding number of cycles leading to failure N. It is usually assumed that the points for N are log-normally distributed – see the standards: American Society for Testing and Materials ASTM E 739 – 91(2006) and Eurocode 3: Design of steel structures - Part 1-9 Fatigue(2006).

For the purpose of the shear strength degradation in the S-N curve, instead of the cyclic stress level σ_{cyc} the ordinate axis is described by a ratio σ_{cyc}/S_0, which is the ratio of the applied deviatoric cyclic stress σ_{cyc} to the deviatoric part of the static strength S_0. The S_0 is given as:

$$S_0 = \sigma_1 - \sigma_3 \tag{1}$$

where σ_1 and σ_3 are the maximum and minimum principal stresses at failure.

The applied cyclic stress is given as:

$$\sigma_{cyc} = \sigma_{max} - \sigma_{min} \tag{2}$$

where σ_{cyc} is the applied cyclic stress level, σ_{max} is the maximum deviatoric cyclic stress and σ_{min} is the minimum deviatoric cyclic stress.

The reason for using the ratio σ_{cyc}/S_0 instead of simply σ_{cyc} is that the shear strength of geomaterials depends on the confining pressure, unlike the properties of metals (see the numerous experiments conducted by Bridgman(1923). In order to be able to compare the loss of the static strength S_0 with the applied cyclic stress σ_{cyc}, the level of the confining pressure has to be taken into account. The tests for a confining pressure of 0 kPa would be similar to tests on concrete (see the procedure in: ACI Committee, 1993) and on steel, but that does not give a full description of the shear strength reduction of geomaterials.

2.2. Remaining strength approach

For the remaining strength approach, a sample is first subjected to a cyclic load σ_{cyc} for a given number of load cycles n. Then, in the last cycle, the sample is loaded until failure.

Since N is the life or the number of cycles until failure, for the remaining strength approach: $n < N$. The predetermined number of load cycles n is given arbitrarily; however, the powers of the number 10 are used to be able to present the results clearer on a semi-logarithmic plot. The theoretical maximum possible value of n (denoted as n_{max}) should be more or less similar to the N value obtained in the S-N tests for the same cyclic stress ratio σ_{cyc}. This would also correspond to the same loss of strength for both the S-N approach and the remaining strength approach ($S_{rem} = \sigma_{cyc}$).

The applied cyclic stress levels σ_{cyc} are the same as for the S-N approach. For each cyclic stress level σ_{cyc}, a single curve can be found. The goal is to describe the remaining strength S_{rem} as a function of the cyclic stress level σ_{cyc}, the number of applied cycles n and the initial static strength S_0, so:

$$S_{rem} = f(\sigma_{cyc}, n, S_0) \tag{3}$$

In the case when $n = 0$, the remaining strength S_{rem} equals the static strength $S_{rem} = S_0$. It was assumed that the remaining strength is a straight line for each cyclic stress level σ_{cyc}, plotted on a semi-logarithmic scale normalised

by the static strength S_0. Based on this, Eq. 3 can be written as:

$$\frac{S_{rem}}{S_0} = A(\sigma_{cyc}, S_0) - B(\sigma_{cyc}, S_0) \cdot \log_{10} n \quad (4)$$

The parameters A and B depend on the cyclic stress σ_{cyc} and S_0, and will be obtained by a linear regression for a semi-logarithmic plot.

A few models have already been proposed in the literature for developing the parameters of remaining strength, see for example: Broutman & Sahu(1972), Reifsnider & Stinchcomb (1986), Gürler (2013), etc. However, these models are more complicated and may not be suitable for geomaterials. Therefore Eq. 4 will be used for comparing the remaining strength model with the S-N curve.

3. Laboratory Testing

3.1 Laboratory equipment

The main components of the triaxial load equipment are presented in Fig. 1. The load frame 28-WF4005 Tritech includes a conventional triaxial cell equipped with an internal load cell and linear transducers for measuring vertical axial displacements. The axial loading capacity is approximately 50 kN, which allows for a deviatoric stress up to 44 MPa on a 38 mm diameter specimen.

The confining pressure is applied by water surrounding the test specimen, which is sealed by the top and bottom plates and a latex membrane. The fluid pressure is applied by a hydraulic actuator and is monitored by a pressure transducer located on the loading frame. The cell pressure levels may vary between 0 and 5 bars and are kept constant during the test.

Figure 1 - Laboratory triaxial machine with pressure controllers.

The static and the cyclic axial loads are applied to the specimen by a servo motor and are monitored by a load transducer. The triaxial servo motor is controlled by a LabVIEW software program written for this purpose. The program was designed to control the load and the data acquisition during cyclic triaxial tests, and to precisely apply the speed of the loading and the level of the cyclic stresses.

3.2. Materials description

The shear strength of geomaterials can be described by the Mohr-Coulomb failure criterion. For the purpose of the laboratory tests, four different kinds of materials were tested (properties are given in Table 1). These are divided into two groups:

a) cohesive

- artificial gypsum
- mortar

b) cohesionless and low-cohesive

- limestone
- sand (crumbled limestone)

All samples had the same diameter d = 38 mm and height h = 78 mm.

The measurement of the loss of strength due to cyclic loading requires many time-consuming tests to be carried out. High accuracy test results would allow reducing the total number of laboratory tests and significantly decrease the testing time. In order to provide a high accuracy of the tests results, highly homogenous material samples are needed. This is not the case, however, for natural geomaterials. The spread of the static and cyclic test results, for natural geomaterials, is usually very high. Therefore, manmade gypsum and mortar samples were used to assure the homogeneity of the materials and therefore consistency of laboratory test results. The results confirmed (see *e.g.* chapter: *S-N approach*) this assumed high accuracy (a value of $r^2 = 0.82$ for artificial gypsum and r^2 = 0.99 for mortar samples was found for static tests).

Table 1 - Material properties.

Material	dry density ρ_d (g/cm^3)	Porosity n (%)	Void ratio e (-)	D_{50} (-)	C_u (-)	C_c (-)	Density of particles ρ_p (g/cm^3)
Artificial gypsum	1.00	-	-	-	-	-	-
Mortar	1.87	-	-	-	-	-	-
Limestone	1.16	54%	-	-	-	-	-
Crumbled limestone	1.20	53%	1.15	0.2	2.24	0.82	2.74

3.3. Cohesive materials – artificial gypsum and mortar

Gypsum standard samples, were first to be tested (Fig. 2). These were made from gypsum blocks, which are used in the construction of non-load bearing partition walls. These gypsum blocks are composed of gypsum plaster and water. Drilling with a boring machine produced 100 mm long samples which were further trimmed to a 78 mm length. Water cooling during drilling was not necessary because the material was very soft, and the samples were completely dry.

Mortar samples were made in laboratory from a mixture of constant proportions of sand, cement and water. The proportions of sand, cement and water, which gave the most suitable results (with high cohesion and a small data point spread), were 3:3:1. The water-cement (*w*/*c*) ratio was set to 0.33 to provide easy flowing and placement of the mixture into a mould.

The mixture was put in the metal mould for one day, and after its removal from the mould, was left to cure for a period of one month according to the norm EN 12390-2:2000 (2000). Altogether, 6 samples were prepared simultaneously in metal moulds (see Fig. 3).

3.4. Cohesionless and low cohesive materials - limestone and crumbled limestone (sand)

The tested sedimentary limestone was a natural material (carbonate sandstone, also known as Marl or "Mergel") obtained from a construction site at the highway tunnel "Geusselt A2" in Maastricht (Fig. 4). The Maastricht Formation, from which the samples were obtained, is a geological formation in Dutch Limburg, Belgian Limburg and its adjacent areas in Germany. The rock belonging to the Maastricht Formation, is locally called "mergel", and is an extremely weak, porous rock consisting of soft, sandy shallow marine weathered carboniferous limestone (which is in fact chalk and calcareous arenite). The used samples were prepared according to the Eurocode 7, Part 2 (2007). However, it was very difficult to obtain adequate samples for testing, due to their easy cracking and crumbling.

The laboratory tests were conducted on a very young and shallow rock layer. The static shear strength parameters were very low: $\phi = 40.2°$ and $c = 37.4$ kPa (see Pytlik & Van Baars, 2015) so it was decided to treat this material as a very soft rock.

Besides this very weak rock, also cohesionless sand was investigated which was obtained from the crumbled limestone and had the form of fine sand. The dry sand samples were prepared by filling the membrane with sand trough a funnel directly into a 38 mm diameter split form. Hereafter, a compaction was done by hand tamping with a steel rod to obtain a density more or less similar to that of the natural state of the crumbled limestone.

3.5. Testing procedure

The triaxial laboratory testing was divided into two steps: 1) Static Triaxial Tests; and 2) Cyclic Triaxial Tests

3.5.1. Step 1 - Static tests

The static tests were standard unsaturated triaxial tests. A series of single load tests were conducted in order to determine the parameters of the Mohr-Coulomb failure criterion. The parameters - the cohesion *c* and the angle of internal friction ϕ - were calculated through a linear least-square regression analysis for the peak stress value.

3.5.2. Step 2 - Cyclic triaxial tests

The cyclic tests were based on multiple loadings and unloadings under a constant cell pressure ($\sigma_2 = \sigma_3$) and a constant strain rate (the speed of the cyclic loading). Three cyclic loadings levels were applied for both the S-N and the remaining strength approach: 40%, 60%, and 80% of the

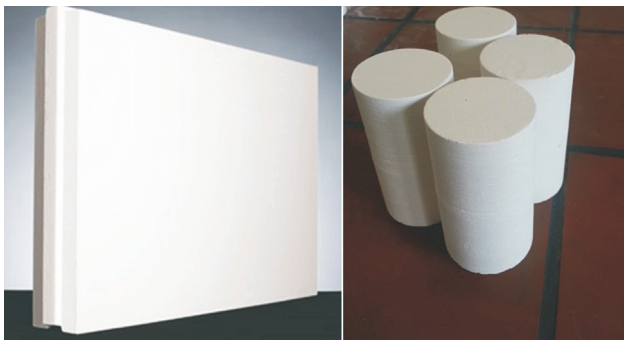

Figure 2 - Artificial gypsum and drilled samples.

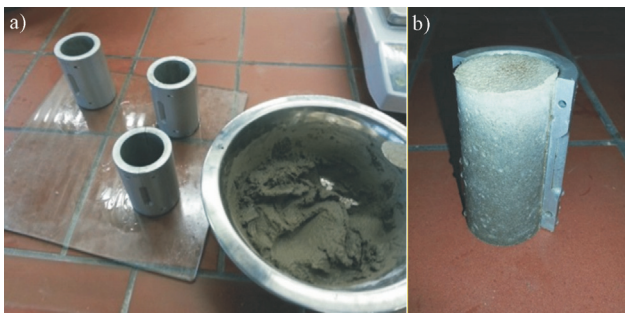

Figure 3 - Mortar samples a) preparation; b) curing.

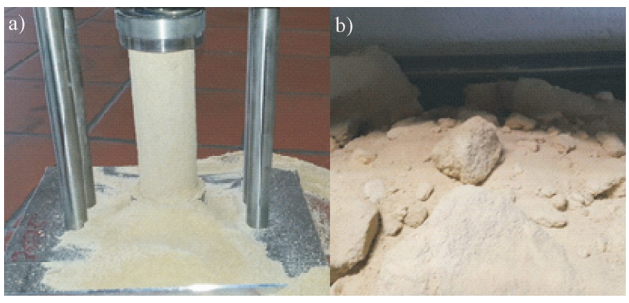

Figure 4 - a) Limestone, b) Crumbled limestone.

maximum static strength. The confining pressure was constant for each test and four values were used 0, 100, 300 and 500 kPa. For all tests, the minimum cyclic loading σ_{min} was equal to 0 kPa, to unload completely the samples. Thus, the cyclic loading is equal to the maximum applied stress:

$$\sigma_{cyc} = \sigma_{max} \quad (5)$$

The σ_{max} can be calculated as follows:

$$\sigma_{max} = \sigma_{1,cyc} - \sigma_3 \quad (6)$$

where $\sigma_{1,cyc}$ is the maximum cyclic principal stress. The $\sigma_{1,cyc}$ is equal to:

$$\sigma_{1,cyc} = \frac{F_{cyc}}{A_s} - \sigma_3 \quad (7)$$

where F_{cyc} is the applied cyclic force, and A_s is the area on which the force F_{cyc} is acting.

The stress ratio R is a parameter for testing steel fatigue, and defined as $\sigma_{min}/\sigma_{max}$. The R had constant value (of 0) for all the tests because $\sigma_{min} = 0$ kPa. The shape of the cyclic loading curve was a typical sinusoidal wave.

The speed of the cyclic loading application (the strain rate) in the triaxial apparatus was set to 0.5 mm/min. This assured a slow cyclic loading frequency ($f = 0.01$ Hz) and an accurate data reading of the force through the LabVIEW software. This also solved the problem of keeping a constant cyclic loading level during the tests, which was an issue for higher frequencies.

4. Laboratory Tests Results

4.1. Tests on cohesive materials

First, the artificial gypsum material was investigated. A total number of 37 cylindrical samples were tested with an unsaturated triaxial test. The obtained static shear strength parameters c and ϕ were compared with the parameters obtained from the cyclic tests. 44 gypsum samples were tested according to the S-N approach and 43 samples according to the remaining strength approach.

4.1.1. S-N approach

Almost all samples selected for the S-N approach were samples which failed prematurely in the remaining strength testing approach (biased samples). Therefore, the accuracy of the S-N approach is questionable. However, for the purpose of a comparison with the remaining strength approach, the results are presented here.

In Fig. 5, a modified S-N plot for the cyclic tests on artificial gypsum is displayed. Additionally, the confidence and prediction bands with a 95% probability have been added, indicating that the uncertainty of the data points spread is high. The spread of the bands is much higher than for metals and for composite materials (*e.g.* the results given by Philippidis & Passipoularidis, 2006). It should also be noticed that the inclination of the curve – how fast does the material lose its strength – is again much higher compared to metals (*e.g.* Manson & Halford, 2006). An endurance limit σ_e (the cyclic loading level at which the material can survive an infinite number of cycles) was not found. This means that, for the cohesive geomaterials presented in this paper, even small loads can cause irreversible damage. More importantly, even for low cyclic stress levels (40% of the initial strength), the life of the artificial gypsum was short, not exceeding 100 000 cycles. Therefore, it can be concluded that cohesive geomaterials are more affected by cyclic loading than metals and composites.

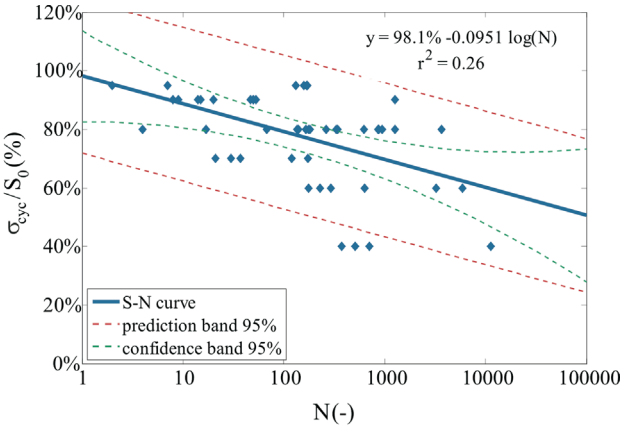

Figure 5 - S-N curve for artificial gypsum samples under cyclic loading.

4.1.2. Remaining shear strength approach

The linear regression lines for different cyclic stress levels (Fig. 6) were forced to intercept the ordinate at 100%. It can be noticed (Table 2 and Fig. 6) that for the remaining strength S_{rem}, the cyclic loading level is unimportant as all lines are very close to each other, and only the number of cycles n is crucial.

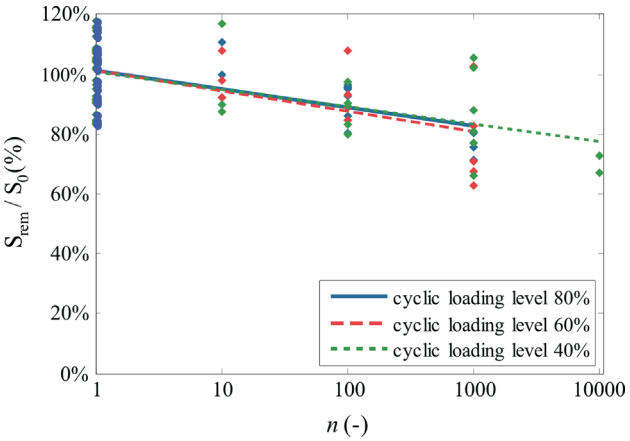

Figure 6 - Remaining strength for artificial gypsum subjected to different cyclic loading levels.

Table 2 - Remaining strength parameters for artificial gypsum subjected to different cyclic loading levels (including static data).

Cyclic loading level	r^2	a	b
40%	0.32	0.068	1.00
60%	0.34	0.086	1.00
80%	0.28	0.072	1.00

If the assumption is made that the strength of the material is greatly dependent on the cyclic level σ_{cyc} then a single log-normal curve for all cyclic tests, with confidence and prediction bands, can be presented. This curve (Fig. 7) fits all samples, both static and cyclic, even though it omits the information about the cyclic loading level. This curve is very similar to the S-N curve. This should be further investigated, because for most materials (*e.g.* composites) different cyclic stress levels cause different reductions in strength. The lack of dependency between the cyclic stress level σ_{cyc} and the remaining strength S_{rem} could be caused by the high scattering of data points, and thus any relationship was hard to find. This also implies that the strength reduction approach loses one of its advantages – the estimation of the life for different cyclic loading ratios. Therefore, the S-N approach seems to be a faster method as it requires fewer tests while giving similar information about the loss of strength as the remaining strength approach. Also, no correlation was found between the remaining strength and the confining pressure σ_3.

The mortar samples gave more accurate static test results than the artificial gypsum samples (higher value of $r^2 > 0.97$). However, the cyclic tests on mortar presented a similar pattern to the results of the artificial gypsum material - with a high spread of cyclic data points (Figs. 8 and 9). Therefore, the high data spread for the S-N approach and the remaining strength approach could be an intrinsic property of cohesive materials. Due to its inhomogeneous internal structure, the cyclic strength results are quite varied.

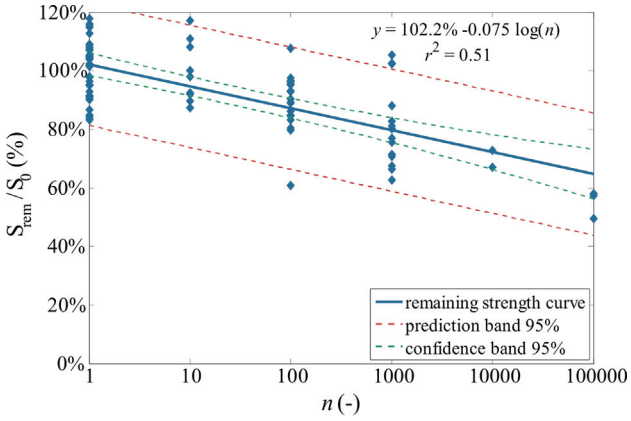

Figure 7 - Remaining strength curve of all cyclic tests for artificial gypsum.

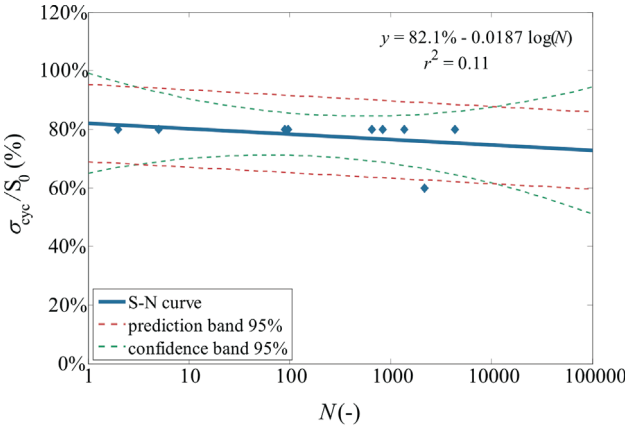

Figure 8 - S-N curve for mortar material.

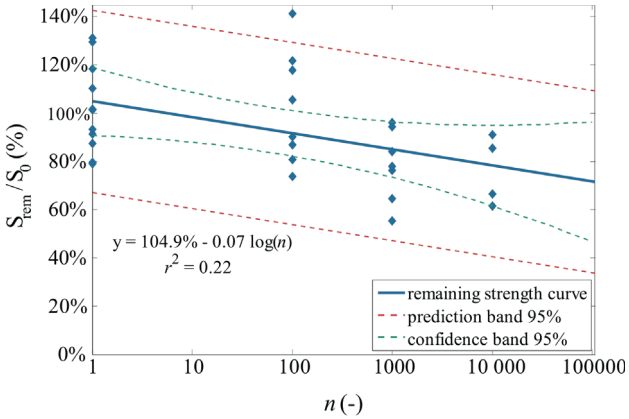

Figure 9 - Remaining strength curve for mortar material.

It was noticed for mortar, that the samples had a longer life than artificial gypsum (based on the S-N approach). This could be related to a higher static strength for mortar than for gypsum ($\phi = 51.4°$, $c = 1.4$ MPa for mortar; and $\phi = 40.9°$, $c = 1.2$ MPa for gypsum). This means that the stronger the material, the longer its life will be, for the same type of cyclic loading.

More importantly, for higher cyclic loading stress levels, a lot of samples failed before reaching the number of predetermined cycles n, before the final loading until failure. Taking into consideration only the remaining samples for the remaining strength approach could result in significantly overestimating of the remaining strength and the life of the material. This is another reason which decreases the usefulness of the remaining strength approach. Moreover, even including the static data points in the remaining strength approach did not increase the accuracy of the model for lower number of cycles (Fig. 7). This could be due to a) the strength reduction being non-linear or b) the logarithmic scale not being the most adequate in terms of shear strength reduction.

4.2. Tests on low-cohesive or cohesionless materials

In order to investigate the fatigue of very weak materials, cyclic triaxial tests were carried out on limestone and on crumbled limestone, with the same procedure as for the cohesive geomaterials. But, due to a low number of available limestone samples, only two cyclic loading ratios were applied: 80% and 40%. Also, the number of applied cycles was rather small – only series of n = 10, 100 and 1000 cycles were carried out. For the remaining strength approach, 9 samples were cyclically loaded (the results are presented in Fig. 10). S-N tests were not conducted due to the lack of samples.

The test results showed that there is no fatigue in limestone at least for a number of cycles up to 1000. The strength of the limestone even increased (Fig. 10). Similar results were found for crumbled limestone and a few other cohesionless geomaterials. The main conclusion regarding the cohesionless and low-cohesive materials is that the strength increases after cyclic loading, due to densification (Youd, 1973). For very dense cohesionless materials, however, the strength can decrease.

The cyclic loading on cohesionless materials, has already been investigated and described by others. The description is usually accompanied by the shakedown theory (*e.g.* by Yu *et al.*, 2007). The basic assumption of the shakedown theory is that below a certain load (named shakedown load) the material will eventually shakedown, *i.e.*, the ultimate response will be purely elastic (reversible) and therefore, there is no more accumulation of plastic strain. If the applied load is higher than the shakedown load, uncontrolled permanent deformations will develop and unstable conditions will progress.

The result for the plastic strain accumulation of the crumbled limestone agrees with the predictions from the shakedown theory. Suiker (2002) found that cohesionless materials influenced by cyclic loading could obtain higher strength parameters than without cyclic loading.

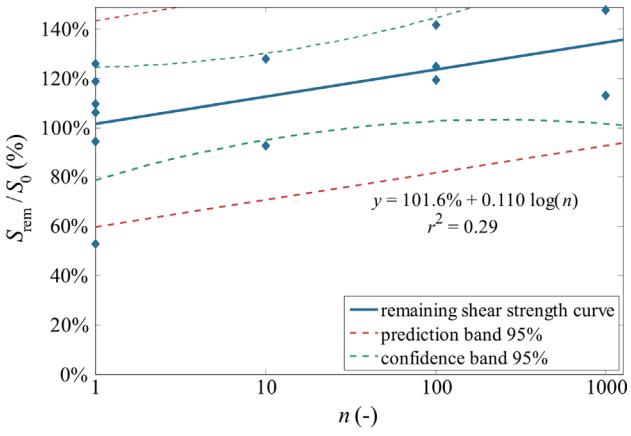

Figure 10 - Remaining strength curve for limestone.

5. Stiffness Degradation

Another interesting phenomenon to investigate is stiffness degradation during cyclic loading, as it requires less laboratory testing than the strength tests, especially because it can be assessed by non-destructive techniques. The stiffness degradation progress can be used as a rough estimation of the material's condition and could improve the assessment of the fatigue life.

One can expect that, a comparison of the initial stiffness E_0 with the stiffness during cyclic loading contains information about the actual life consumption of the sample. Unfortunately, only small number of tests has been conducted on the stiffness degradation for geomaterials, and thus there is not enough reference data and no constitutive model. One of the few examples is offered by Bagde & Petros (2011), who observed the degradation of the stiffness modulus in compressional cyclic tests on sandstone samples.

For the purpose of this investigation, the proportional maximum and minimum limits were taken as 90% and 10% of the maximum strength. The 10% limit was chosen because for lower stresses the readings of the stiffness were not accurate enough. The ratio E_{rem}/E_{max} is denoted as the ratio of the stiffness in the last cycle E_{rem} to the maximum stiffness E_{max} during the whole cyclic loading test. The whole cyclic test run was taken into consideration, as for the first few cycles the stiffness can vary significantly (see Figs. 11 and 13) and the maximum stiffness is not found necessarily at the very beginning. The stiffness data was obtained from the same tests as for the remaining strength approach, because the strains were also measured during these tests.

The cohesive materials lose their stiffness with an increase in the number of cycles, as can be noticed from Fig. 11. The stiffness degradation plot for artificial gypsum, see Fig. 12, is very similar to the corresponding remaining strength plot of artificial gypsum (compare Fig. 7 with Fig. 12).

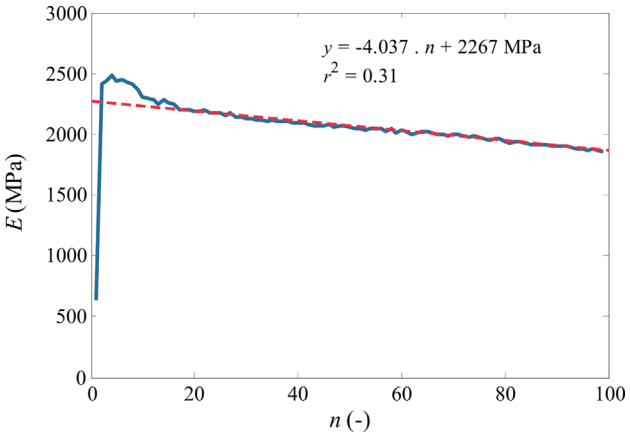

Figure 11 - Stiffness degradation of artificial gypsum sample (100 cycles).

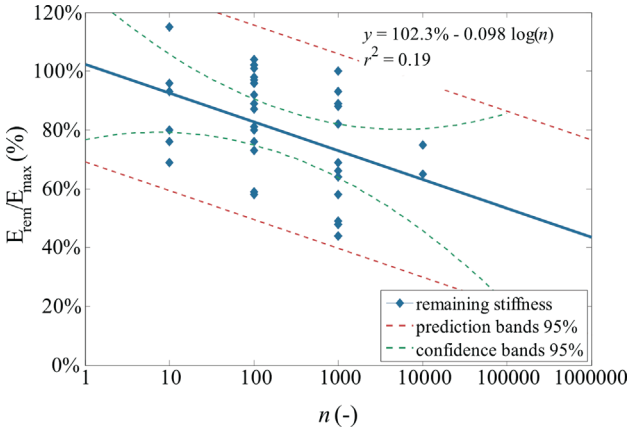

Figure 12 - Stiffness degradation curve for artificial gypsum.

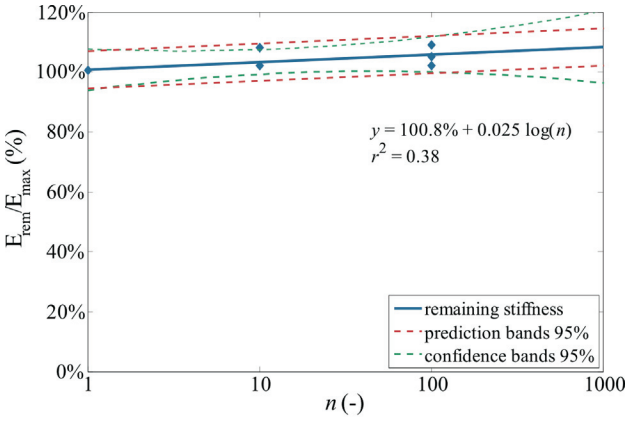

Figure 14 - Stiffness "degradation" curve for limestone.

For the low-cohesive materials, it was found that the cyclic loading induced an increase in stiffness, as can be seen in Fig. 13. This also corresponds to the results from the remaining strength tests on the limestone (compare Fig. 10 with Fig. 14).

It can be concluded that, in terms of stiffness reduction, the stiffness changes in cyclic loading are very similar to the shear strength changes. For cohesive materials under cyclic loading, the stiffness decreases; and for cohesionless materials, the stiffness increases. Fortunately, this will be easy to use in practice, because the stiffness reduction is even more significant than the reduction in strength.

6. Parametrisation of a Remaining Shear Strength Model

For a simple shear strength reduction model, the most convenient would be that the parameter which is affected by cyclic loading is only the cohesion c, while the friction angle ϕ remains constant. This assumption of a constant friction angle ϕ was also formulated in the laboratory tests. Vyalov (1978) stated that for rocks, the decrease of strength over time is a result of a decrease in the cohesion c while the friction angle ϕ remains constant. This corresponds with a statement from Van Baars (1996) who, based on discrete element modelling, stated that the static strength of a cohesive material depends on the contact strength and the normal force distribution.

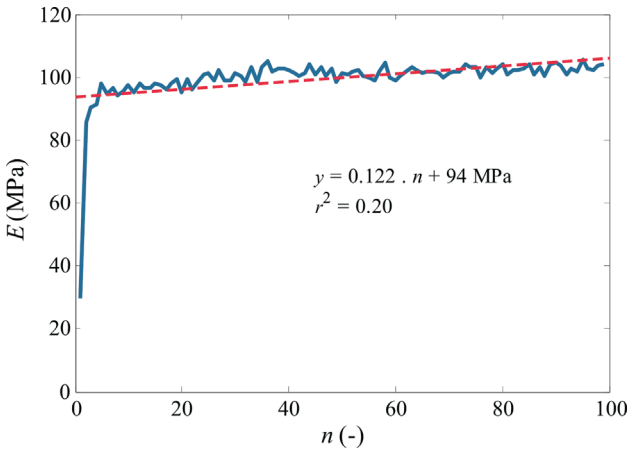

Figure 13 - Stiffness changes of limestone (100 cycles).

Furthermore, Brantut *et al.* (2013) gave a summary of his tests, proving that brittle creep, which is defined by him as permanent deformation due to mechanical stress, reduces the cohesion of rock, but this does not directly affect their internal friction. This indicates that failure which is extended over time is mainly related to reduction of the cohesion. The results of the laboratory tests presented herein also indicate that the cohesive materials lose their strength, while the cohesionless materials do not.

Based on this constant friction angle, one can make a plot, similar to that of the remaining strength - Fig. 5 and, for the S-N approach, Fig. 7 - , in which the remaining strength ratio S_{rem}/S_0 or cyclic stress ratio σ_{cyc}/S_0 is replaced by the remaining cohesion ratio c_{rem}/c.

For each of the tests, the remaining cohesion c_{rem} is obtained by recalculating the cohesion with the Mohr-Coulomb equation. The remaining cohesion for a single test can be calculated from the formula:

$$c_{rem} = \left(\frac{\sigma_1 - \sigma_3}{2}\right)\frac{1}{\cos\phi} - \left(\frac{\sigma_1 + \sigma_3}{2}\right)\tan\phi \qquad (8)$$

where, σ_1 and σ_3 correspond to the maximum and minimum principal stresses at failure.

The interpolated formula of the remaining cohesion can be written as:

$$c_{rem} = c \cdot [B - A \cdot \log(n)] \qquad (9)$$

where A and B are constant parameters obtained from the regression line, and are specific to the material.

In Eq. 9, the parameter which would describe the cyclic loading level is not given. This is because it was found from the laboratory tests for the remaining shear strength approach, that the strength reduction was independent from

the cyclic loading level. This requires further investigation however, as mentioned before, because this independency is unexpected.

For the S-N approach, the c_{rem} is obtained in the same way; but, the constants E and F are different here:

$$c_{rem} = c \cdot [F - E \cdot \log(N)] \quad (10)$$

For the cohesionless materials (*e.g.* sand) no cohesion is present (c = 0 kPa, or it is very low); thus, the shear strength reduction can be neglected for such a material (although the cyclic strain accumulation should be checked anyway). Therefore, a clear distinction has to be made between the cohesive and the cohesionless cyclic behaviour.

For cohesive cyclic behaviour, the updated shear strength τ can be given as:

$$\tau = \sigma \tan \phi + c_{rem} \quad (11)$$

where the degraded cohesion c_{rem} replaces the "static" cohesion c. Implementing Equation 9 in Eq. 11 yields for the number of applied cycles n (or N):

$$\tau = \sigma \tan \phi + c \cdot [B - A \cdot \log n] \quad (12)$$

In terms of the maximum and minimum principal stresses σ_1 and σ_3, the Mohr-Coulomb failure criterion can then be proposed as:

$$\left(\frac{\sigma_1 - \sigma_3}{2}\right) - \left(\frac{\sigma_1 + \sigma_3}{2}\right) \sin \phi - c_{rem} \cdot \cos \phi = 0 \quad (13)$$

In order to describe fully the fatigue of geomaterials, one needs to give the life of a material for the remaining strength approach. The number of cycles before failure (life) for the remaining strength approach $n_{max} = N$ can be found from some simple transformations of Eq. 9:

$$\log_{10} n_{max} = \frac{c \cdot b - c_{rem}}{c \cdot a} \quad (14)$$

and finally:

$$n_{max} = N = 10^{\frac{c \cdot b - c_{rem}}{c \cdot a}} \quad (15)$$

To calculate the reduced strength for a combination of different level and number of cyclic loads, an additive rule is needed. Care must be taken to use *e.g.* the simple additive Palmgren-Miner rule, which is the most popular in metal fatigue. This rule could lead, however, to an unsafe foundation because it underestimates the damage at very low load levels and it does not predict well the applied load sequences. Future tests should be conducted to confirm whether the methods from metal fatigue (*e.g.* Palmgren-Miner rule) can be applied for describing the impact of various cyclic loadings in geomaterials.

7. Advantages and Disadvantages of the S-N and Remaining Shear Strength Approach

The biggest advantage of the remaining strength approach, compared to the S-N and the damage accumulation approach (*e.g.* the Paris law), is that the remaining strength approach does not only predict the number of cycles until failure, but gives an indication of the remaining strength as well. The remaining strength is measured directly and in a simple way, and the empirical damage accumulation rule (*e.g.* the Palmgren-Miner linear damage rule) can be replaced by a physical parameter – the shear strength.

Since the number of cycles n is controlled for the remaining strength approach, the laboratory tests for this approach can be easily scheduled, as the time of one cycle is known from the static tests. For the S-N approach it is difficult to predict the life-time of a sample before having finished some of the other cyclic tests. Therefore, the time planning for the S-N approach is more complex.

Another advantage of the remaining strength approach is that the static tests can be included. It was found however, that these results did not necessarily improve the accuracy compared to the S-N curve.

The biggest disadvantage of the remaining strength approach is that it only takes into account the samples which survived the applied number of cyclic loads n. This leads to the conclusion that the remaining strength approach overestimates the strength compared to the S-N approach, and therefore the correlation of the remaining strength approach is questionable. Thus, the standard S-N approach offers more reliable results, and also requires less testing.

For both approaches, the big spread of the resulting data implies that a lot of samples have to be tested to obtain a good accuracy for geomaterials. Unfortunately, these tests are very time consuming.

8. Conclusions

Cyclic loading on geomaterials investigated in this paper can cause different types of effects: for example, the shear strength of crumbled limestone increases during cyclic loading, while for cohesive materials the strength decreases (fatigue). This can be seen as a degradation of the cohesion. The most significant factor in the cohesion reduction was found to be the number of applied cycles.

The fatigue of cohesive geomaterials presented in this paper can be fully described by the remaining cohesion. The existence of a constant friction angle was demonstrated in different ways, for example by tests on low-cohesive and cohesionless materials where the friction angle under cyclic loading was not reduced. Some tests even showed an increase of the value of the friction angle due to densification. Care must be taken however, because the number of tests and the set of investigated materials were limited and the r^2 value in the cyclic tests was rather low.

The amplitude of the cyclic loading does not affect the remaining strength. Also the confining pressure does not affect the remaining strength. Therefore, the remaining strength model proposed in this paper is both simple and effective.

The strength degradation can be linked to the stiffness degradation, which shows a similar pattern. For practical purposes, this could help to estimate the reduction in strength by non-destructive methods, based on changes in the stiffness.

Both the S-N and the remaining strength approach have their advantages and disadvantages. The S-N approach offers, however, a faster and safer solution compared to the remaining strength approach.

References

ACI Committee 2015 (1993). Consideration for design of concrete structures subjected to fatigue loading - ACI 215R-74. In ACI Manual of Concrete Practice Part 1 – 1993, American Concrete Institute, Detroit, pp. 1-24.

American Petroleum Institute (2000). Recommended Practice for Planning, Designing and Constructing Fixed Offshore Platforms—Working Stress Design. API Recommended Practice 2A-WSD (RP 2A-WSD), Washington, 60 p.

Andersen, K.; Puech, A. & Jardine, R. (2013). Cyclic resistant geotechnical design and parameter selection for offshore engineering and other applications. Proceedings of TC 209 Workshop – Design for cyclic loading: piles and other foundations, 18 ICSMGE, Paris, pp. 9-44.

ASTM (2006). E 739-91 - Standard Practice for Statistical Analysis of Linear or Linearized Stress-Life (S-N) and Strain-Life (e-N) Fatigue Data. ASTM, Philadelphia, pp. 1-7.

Bagde, M. & Petros, V. (2011). The Effect of Micro-Structure on Fatigue Behaviour of Intact Sandstone. International Journal of Geoscience, 2:03, pp. 240-247.

Brantut, N.; Heap, M.; Meredith, P. & Baud, P. (2013). Time-dependent cracking and brittle creep in crustal rocks: A review. Journal of Structural Geology, 52:17-43.

Bridgman, P.W. (1923). The compressibility of thirty metals as a function of temperature and pressure, Proceedings of the American Academy of Arts and Science, 58:165-242.

Broutman, L. & Sahu, S. (1972). A new theory to predict cumulative fatigue damage in fiberglass reinforced plastics. Composite Materials: Testing and Design (Second Conference). ASTM STP 497 American Society for Testing and Materials, Philadelphia, pp. 170-188.

DeAlba, P.; Seed, H. & Chan, C. (1976). Sand Liquefaction in Large Scale Simple Shear Tests. Journal of the Geotechnical Engineering Div., 102(GT9), pp. 909-927.

DNV (2013). Design of Offshore Wind Turbine Structures. Det Norske Veritas, Oslo.

EN (2000). 12390-2:2000 - Testing Hardened Concrete. Part 2: Making and Curing Specimens for Strength Tests. CEN, Brussels.

EN (2006). 1993-1-9:2006 Eurocode 3 - Design of steel structures – Part 1-9: Fatigue. CEN, Brussels.

EN (2007). 1997-2 Eurocode 7 - Geotechnical Design, Part 2: Ground Investigation and Testing. CEN, Brussels.

EN (2004). 1998-5: Eurocode 8 - Design of structures for earthquake resistance – Part 5: Foundations, retaining structures and geotechnical aspects. CEN, Brussels.

Gürler, S. (2013). The mean remaining strength of systems in a stress-strength model. Hacettepe Journal of Mathematics and Statistics, 42:2, Ankara, pp. 181-187.

Ibsen, L. (1999). Cyclic Fatigue Model. AAU Geotechnical Engineering Papers: Soil Mechanics Paper, 34:R9916, Aalborg, pp. 1-30.

Lee, K. & Albesia, A. (1974). Earthquake induced settlements in saturated sands. Journal of Geotechnical Engineering ASCE, 100:04, pp. 387-405.

Manson, S. & Halford, G. (2006). Fatigue and Durability of Structural Materials. ASM International, Ohio, pp 123-156.

Matlock, H.; Foo, S.H. & Bryant, L.L. (1978). Simulation of lateral pile behaviour. Proceedings of Earthquake Engineering and Soil Dynamics, ASCE, New York, pp. 600-619.

Niemunis, A., Wichtmann, T. and Triantafyllidis, T. (2005). A high-cycle accumulation model for sand, Computers and Geotechnics, 32:4, pp. 245-263.

Philippidis, T. & Passipoularidis, V. (2006). Residual strength after fatigue in composites: Theory *vs.* experiment. International Journal of Fatigue, 29, pp. 2104-2116.

Pook, L. (2007). Metal Fatigue. Springer, Dordrecht, pp. 35-65.

Pytlik, R. & Van Baars, S. (2015). Triaxiaalproeven op Limburgse mergel leveren verrassende resultaten (in Dutch). Geotechniek, 19(3), Rotterdam, pp. 10-13.

Reifsnider, K.L. & Stinchcomb, W.W. (1986). A critical Element Model of the Residual Strength and Life of Fatigue-Loaded Composite Coupons. Proceedings of the Conference on Composite Materials: Fatigue and Fracture, Philadelphia, pp. 298-303.

Seed, H.B. & Lee, K. (1966). Liquefaction of saturated sands during cyclic loading. Journal of Soil Mechanics and Foundation Engineering, 92(SM6), pp. 105-134.

Seed, H.B., Martin, P., & Lysmer, J. (1976). Pore water pressure changes during soil liquefaction. Journal of the Geotechnical Engineering Division, 102(GT4), pp. 323-346.

Suiker, A. (2002). The Mechanical Behaviour of Ballasted Railway Tracks. Delft University of Technology, Delft, pp. 127-159.

Van Baars, S. (1996). Discrete Element Analysis of Granular Materials. Delft University of Technology, Delft, pp. 61-81.

Vyalov, S. (1978). Rheologic Principles of Soil Mechanics (in Russian). Vysshaya Shkola, Moscow. pp. 285-338.

Youd, T. (1973). Factors controlling maximum and minimum densities of sand. ASTM Special Technical Publications, 523, American Society for Testing and Materials, Philadelphia, pp. 98-112.

Yu, H.; Khong, C. & Wang, J. (2007). A unified plasticity model for cyclic behaviour of clay and sand. Mechanics Research Communications, 34(2):97-114.

List of Symbols

a, b, A, B, and F, E: constants obtained in linear regression

c: cohesion

c_{rem}: remaining cohesion

d: diameter of a sample

h: height of a sample

n: predetermined number of applied load cycles

n_{max}: maximum number of load cycles

A_s: cross-sectional area of a sample

E_{rem}: remaining stiffness

E_{max}: maximum stiffness in the whole test run

F_{cyc}: applied cyclic force

N: life of a sample (the number of cycles until failure)

S_0: static strength

S_{rem}: remaining strength

ϕ: internal friction angle

σ_1: maximum principal stress

σ_3: minimum principal stress

σ_{cyc}: cyclic stress level

$\sigma_{1,cyc}$: maximum cyclic principal stress

σ_{max}: maximum deviatoric cyclic stress

σ_{min}: minimum deviatoric cyclic stress

τ: shear strength